Fabrication of High Chromium Cast Iron/Hadfield Steel Composite Materials by the Hot Rolling Process

Guofeng YUAN [1] *, Fei ZHAO [1], Guijun WU [1, 2]

[1] *School of Mechanical Engineering, Anyang Institute of Technology, Anyang, China*
[2] *Department of Mechanics Engineering, Kyrgyz State Technical University Named After I. Razzakov, Aitmatov av., 66, Bishkek 720044, Kyrgyzstan*

http://doi.org/10.5755/j02.ms.39300

Received 31 October 2024; accepted 5 February 2025

Bimetal composite blanks were successfully prepared from high chromium cast iron (HCCI) and Hadfield steel by the hot-rolling process. The macrostructure and microstructure of the composite were investigated. After hot-rolling formation, the hard HCCI layers were fractured and embedded in ductile Hadfield steel, forming a three-dimensional composite structure. The two metals were fused and no defects such as interface cracks or unbonded areas were found. A metallurgical bonding between Hadfield steel and HCCI was revealed. The kernel average misorientation (KAM) value of the Hadfield steel layer was low, while the HCCI layer showed a larger green area. It indicated that the HCCI layer had high strain energy and high dislocation density. The bonding process of two metals includes three stages: physical contact, physico-chemical bonding and mutual diffusion.
Keywords: high chromium cast iron, Hadfield steel, hot-rolling, microstructure.

1. INTRODUCTION

Wear-resistant materials are in great demand in metallurgy, mining, electric power, and other industries due to their impact-, wear- and corrosion-resisting properties in service [1, 2]. Wear-resistant materials are generally required to have both good wear resistance and good impact toughness [3]. High chromium cast iron (HCCI) is often used in the preparation of hammers, liners, grinding balls, and other wear parts. HCCI can be divided into eutectic, hypereutectic, and hypoeutectic types according to the chemical composition, and specifically, the type is determined by the mass fractions of Cr and C elements [4 – 6]. Compared with ordinary cast iron, HCCI has good wear and corrosion resistance. Under wear conditions, the wear resistance of HCCI increases with the increase of the volume fraction of eutectic carbides. However, a large volume fraction of eutectic carbides can impair the toughness of HCCI, leading to high crack sensitivity and early component failure, especially under high-speed impact [7, 8]. To improve the mechanical properties of HCCI and enhance its engineering application value, researchers often adopt heat treatment [9], alloying [10] and changing the casting process to improve the comprehensive mechanical properties of HCCI.

As a kind of wear-resistant material, Hadfield steel shows a rapid work hardening rate on its surface under the action of a large impact load or a large contact stress, while its inner austenite maintains good toughness. However, under small and medium impact loads, the work hardening rate of the surface layer of Hadfield steel is slow, and its wear resistance is poor, not comparable to that of HCCI and other low alloy wear-resistant steel [12, 13]. Various pre-hardening methods have been developed and used to improve the wear resistance of Hadfield steel under small and medium loads [14, 15].

How to prepare wear-resistant materials with both high hardness and good toughness is the focus of current research. Bimetallic composites can effectively combine the performance advantages of dissimilar metals, thus presenting a good application prospect in modern engineering field [16 – 18]. At present, surface cladding [19], casting [18], hot pressure diffusion [20, 21], and supersolidus liquid-phase sintering methods are commonly used to compound HCCI with low-carbon alloy steel [22]. Niu et al. [15] fabricated the composite of HCCI bars/Hadfield steel by inserting the preform of high chromium alloy powder flux-cored wires into high manganese steel melt. Xie et al. [20] fabricated the HCCI/low carbon steel composite material by cast and hot rolling process. These methods effectively combine the performance advantages of the two metals. With the advantages of high efficiency, low cost and mass production, the hot-rolling bonding method has been widely applied to the preparation of bimetal composites [16]. At present, there is little research on the preparation of HCCI/Hadfield steel bimetallic composites by the hot-rolling process. In the present paper, the composites consisting of wear-resisting HCCI and Hadfield steel with good toughness were prepared by the hot-rolling formation method, and their macroscopic morphology and microstructure were studied.

2. EXPERIMENTAL PROCEDURE

The raw materials used in this study are commercial Hadfield steel plates and as-cast HCCI plates. The main composition of the two metals is listed in Table 1.

* Corresponding author: G.F. Yuan
E-mail: *20160934@ayit.edu.cn*

Table 1. Chemical compositions of HCCI and Hadfield steel, wt.%

Material	C	Si	Cr	Mn	P	S	Mo	Ni	Al	Fe
HCCI	2.75	1.05	26.5	0.90	0.02	0.02	0.05	0.40	–	balance
Hadfield steel	0.95	0.44	–	12.67	0.01	0.002	–	–	0.038	balance

The Hadfield steel material used consists of 12.67 wt.% manganese, with good toughness and work hardening properties. The HCCI used has high carbon content, mainly composed of hexagonal primary M_7C_3 carbides and the austenite matrix, as shown in Fig. 1. These hard carbides endow HCCI with good wear resistance but also weaken its mechanical properties and narrow its application range [23].

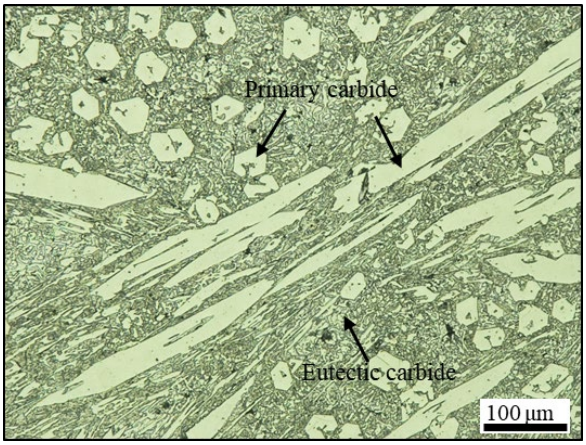

Fig. 1. Optical micrograph of HCCI

The dimensions of Hadfield steel and HCCI are 150 × 100 × 3 mm and 150 × 100 × 2.5 mm, respectively. A steel wire brush was used to polish the surface of the plates to remove impurities, stains and oxidized layers. Through mechanical grinding of plate surfaces, surface roughness was enhanced, and fresh metal was exposed. In this way, two metals bound better to each other. After cleaning, the plates were stacked alternately, with the top and bottom layers being Hadfield steel plates, as shown in Fig. 2. In this study, three-, five- and seven-layer stacking methods were used. The stacked slabs were welded, sealed, vacuumed, homogenized at 1100 ℃ for 0.5 h and finally hot-rolled at 1000 – 1100 ℃, with the rolling rate of 0.1 m s^{-1}. The three kinds of stacked slabs were rolled into 6mm-thick sheets by multi-pass rolling. After hot-rolling formation, the composite billets were air-cooled to room temperature.

The metallographic specimens were machined, ground, polished and etched with a 4 % nitric acid-ethanol solution for 30 – 40 s. The microstructure of the composite was analyzed using an optical microscope (OM) and a scanning electron microscope (SEM) equipped with an energy dispersive spectroscope (EDS) and electron backscatter diffraction (EBSD). The EBSD specimens were ground, polished and Ar ion-milled for 30min. EBSD measurements were performed at an electron beam angle of 70° and a scanning step of 0.5 μm.

3. RESULTS AND DISCUSSION

3.1. Macrostructure of the composite

Due to the high-volume fraction of hard brittle M_7C_3 carbides in HCCI, cracks propagated and extended fast along the hard and brittle Cr-carbide phase in the process of thermal mechanical deformation. Many macroscopic cracks perpendicular to the rolling direction were formed on the surface of HCCI after hot-rolling deformation, as shown in Fig. 3 a. During multi-pass rolling, the cracks in HCCI layers were filled by Hadfield steel with good plasticity and fluidity, and a new wear-resistant composite material with hard HCCI particles dispersed in the Hadfield steel matrix was prepared.

In order to facilitate direct observation of the distribution of the two materials, the specimens were cut by wire cutting in the middle position of the formed plate along the rolling direction. Fig. 3 b – d shows the macromorphology of the composite slab after hot rolling. It is evident that the continuous layered structure formed by HCCI and Hadfield steel, which exists in the initial billet, is no longer visible. Under the effect of large cumulative deformation, the HCCI layers with poor plastic deformation ability were necked and broken into non-uniform blocks or granules, which were finally completely wrapped by Hadfield steel. The two metals formed a new three-dimensional composite structure. The HCCI/Hadfield steel composite can combine the performance advantages of HCCI and Hadfield steel, that is, high hardness of HCCI and good toughness and work hardening properties of Hadfield steel.

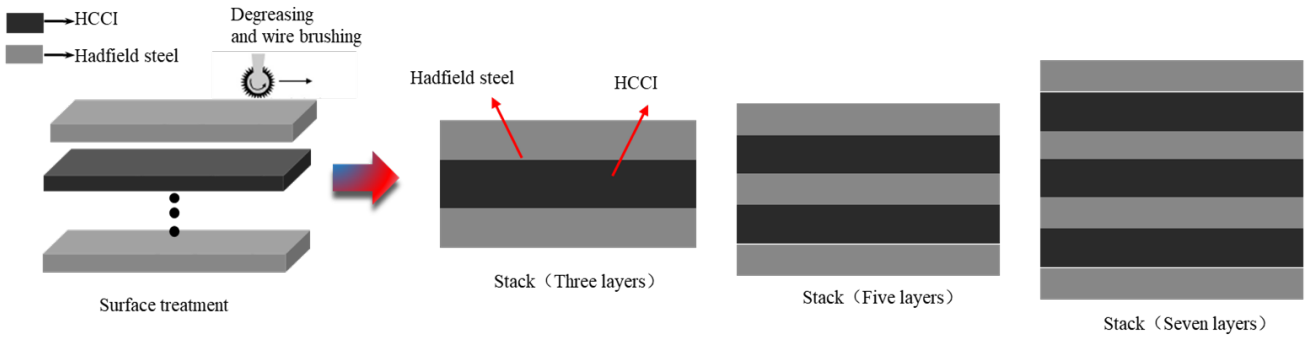

Fig. 2. Schematic diagram of the billet surface treatment and stacking

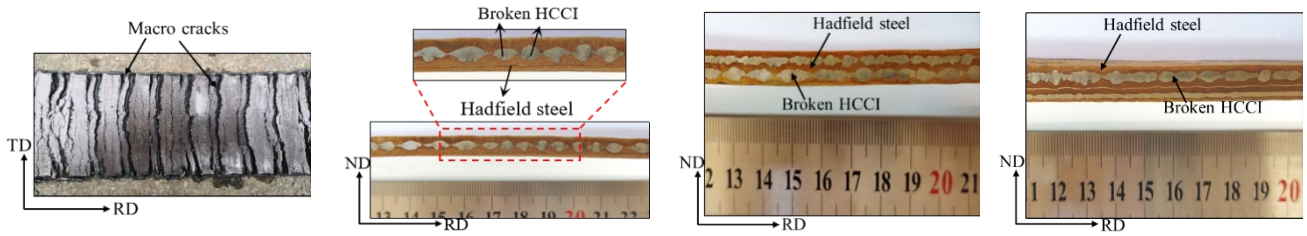

a b c d

Fig. 3. Macromorphology of the sheet after hot rolling: a – single HCCI; b – three layer slab; c – five layer slab; d – seven layer slab

3.2. Microstructure of the composite

The bonding properties of two metals in bimetallic composites have an important effect on the comprehensive mechanical properties of the composites. In this paper, the microstructure of bimetal composite plates prepared by three- and five-layer stacking methods was analyzed. Fig. 4 shows the microstructure of the composite near the interface. In Fig. 4, the upper side is HCCI, and the bottom side is Hadfield steel. The two metals were fused, with no defects such as interface cracks or unbonded areas detected.

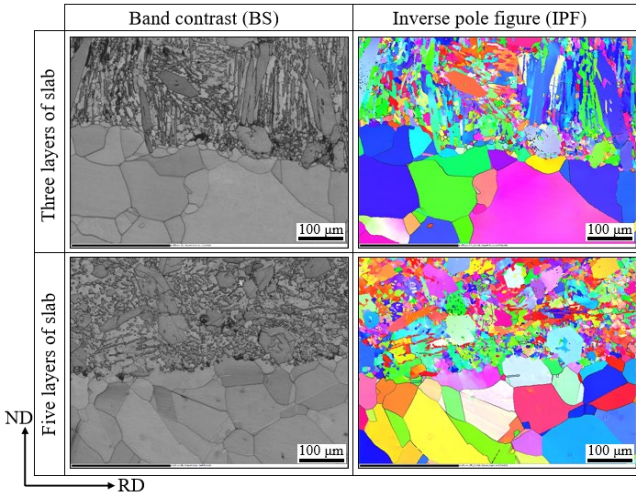

Fig. 4. Microstructure of the composite near the interface

Due to the large plastic deformation at the interface of the two metals in the process of hot-rolling deformation and the large difference in deformation resistance between the two metals, the bonding interface presented different degrees of undulation. The number of grains at the bonding interface decreased, which was mainly attributed to grain recrystallization at higher rolling temperature and larger plastic deformation [24]. Grain refinement at the bimetal bonding interface contributed to the improvement of the bonding strength of the two metals, and smaller grain size was also conducive to the diffusion of elements at the interface under the larger cumulative strain [24, 25].

EDS scanning analysis of the area near the interface of the HCCI/Hadfield steel composite was made, and the results are shown in Fig. 5 and Fig. 6. Different content of elements in the two metals resulted in a concentration difference at the interface. Cr, Mn and Si elements were diffused in the interface region of the two metals. The content of these elements was distributed in a gradient manner on both sides of the interface, and the diffusion distance of elements at the interface was about 10 – 15 μm. This condition further indicates that the two metals have formed a metallurgical bonding at the interface. The mutual diffusion of elements at the bonding interface promotes the metallurgical bonding of the two metals [9, 16].

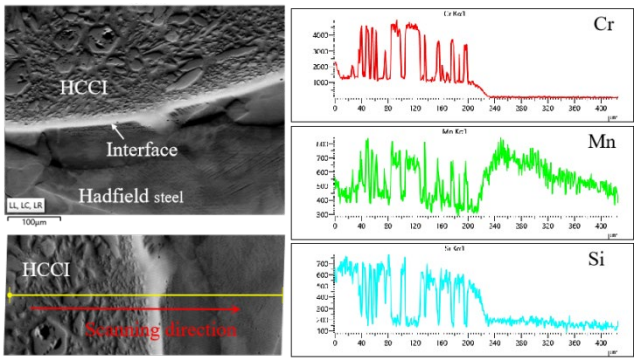

Fig. 5. Results of EDS line analysis of the bonding interface of two metals

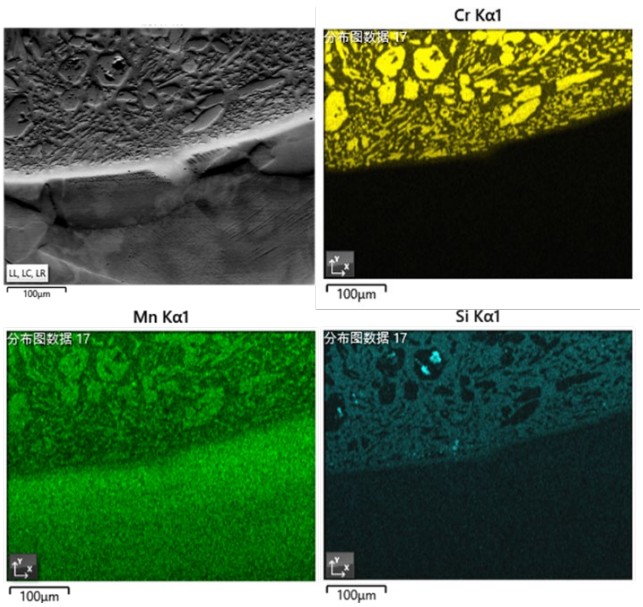

Fig. 6. Results of EDS map analysis of the bonding interface of two metals

The EBSD technique was used to analyse the region near the interface of HCCI and Hadfield steel, and the results are shown in Fig. 7. Fig. 7 a, d shows the phase distribution at the interface of the two metals. In the diagram, blue is the fcc structure, red is the bcc structure, and yellow is the M_7C_3 carbide.

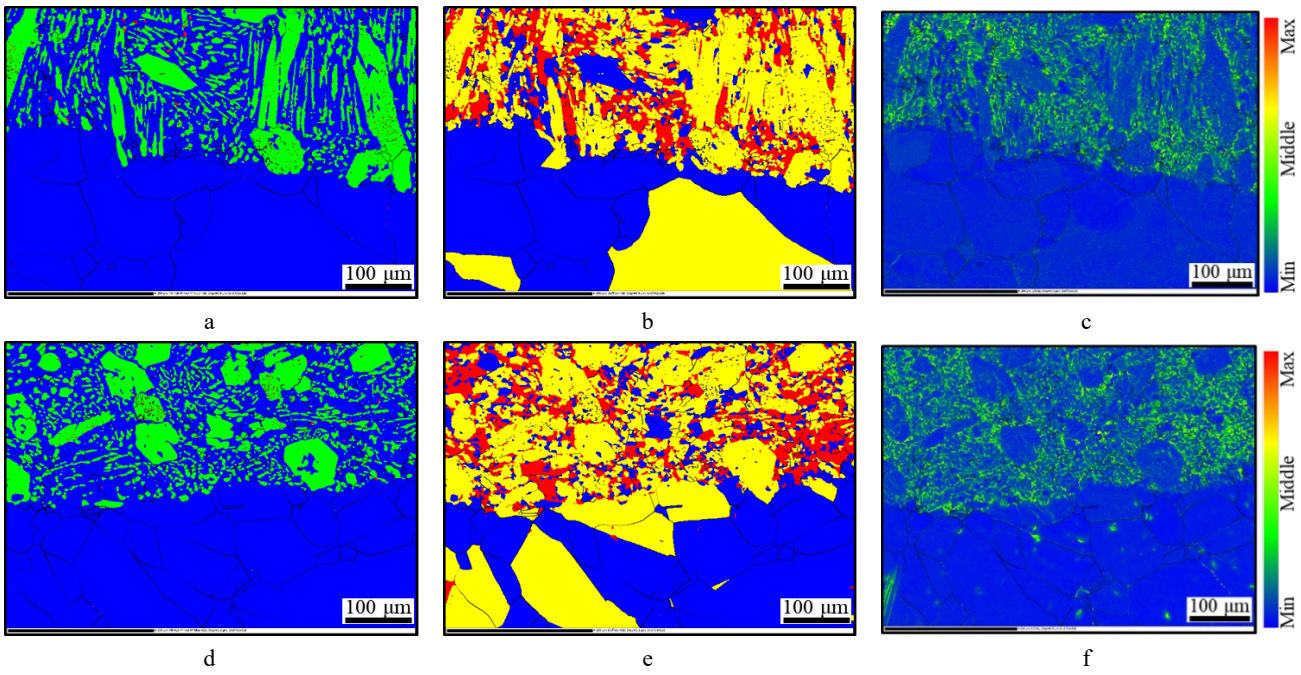

Fig. 7. EBSD analysis of the composite: a, d – phase map; b, c – recrystallization; c, f – kernel average misorientation (KAM) map

HCCI is composed of fcc austenite, the M_7C_3 carbide and a small amount of bcc martensite. Fcc austenite is the primary component of Hadfield steel. Near the interface, fcc austenite in HCCI was integrated with austenite in Hadfield steel, and the hard Cr-carbide in HCCI extruded into the austenite in Hadfield steel, thus improving the binding property of the two metals. Fig. 7 b, e shows the recrystallization diagram at the interface of the two metals. In the figure, blue is the recrystallization structure, red is the deformation structure, and yellow is the substructure. The fcc austenitic phase in Hadfield steel is mainly recrystallized structures and substructures, while that in HCCI is mainly metamorphic structures and substructures.

In the process of thermal deformation, there was a competition between work hardening and dynamic softening in the metals. The kernel average misorientation (KAM) value is an indirect indicator of the degree of plastic deformation in different regions of the material. A larger KAM value often indicates more plastic deformation or a higher dislocation density in this region [26]. The KAM value of the Hadfield steel layer was low, while the HCCI layer had a larger green area, which indicates that the HCCI layer has high strain energy and high dislocation density.

3.3. Forming and bonding mechanism of the composite

In multi-layer rolling, the large cumulative deformation amount and the difference of thermoplastic deformation properties of the two metals lead to the formation of bimetallic composite materials with one metal as the matrix and the other metal as the reinforcement phase. The multi-pass hot-rolling deformation process of the composite material is complicated and can be simplified into three stages, as shown in Fig. 8. Firstly, the two metals made physical contact. Due to mechanical grinding to remove the oxide and oil on the slab surface before rolling, the surface to be bonded had a certain roughness, and there were many scratches, bumps and pits on it. Under the action of the rolling force, the two metals formed an initial bonding, and the micro-holes between the surfaces gradually closed. The two materials were nested at the interface to form an initial mechanical bite.

The second stage is physicochemical bonding. With the increase of rolling deformation, the HCCI layers in the slab were necked and fractured. Hadfield steel at the crack edge was squeezed into the crack in HCCI under the action of roll pressure.

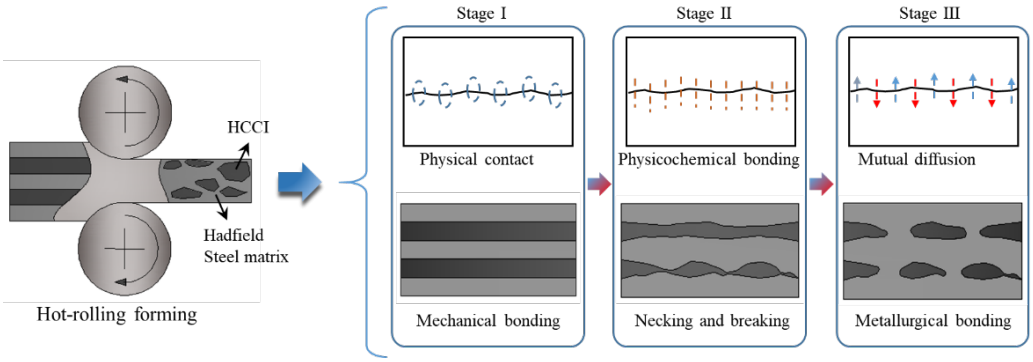

Fig. 8. Diagram of the forming and bonding process of the composite

At the same time, oxides were removed from the surface of the two metal slabs, exposing more fresh metals and thus enhancing physical and chemical effects. Lastly, the two metals were mutually diffused and formed a metallurgical bonding. In this stage, the fractured HCCI was completely wrapped by adjacent Hadfield steel layers, and the two metal materials were completely joined. Broken HCCI and ductile Hadfield steel were connected to form a three-dimensional composite structure. Under the joint action of high temperature and high pressure, the elements in the two metals further diffused into each other, forming a good metallurgical combination.

4. CONCLUSIONS

In this work, the HCCI/Hadfield steel composite blank was successfully fabricated through the hot-rolling process. The macrostructure, microstructure and bonding mechanism of the composites were analysed. The brittle HCCI material was fractured and embedded in ductile Hadfield steel, forming a new type of composite material. The two metals bonded closely and formed a metallurgical bonding. Cr, Mn and Si elements were diffused in the interface region of the two metals with the diffusion distance of about 10 – 15 μm. After hot-rolling forming, high strain energy and high dislocation density were accumulated in HCCI layer. The bonding of the two metals experienced 3 stages, which were physical contact, physicochemical bonding and mutual diffusion.

Acknowledgments

This work was funded by the Key scientific research projects of colleges and universities of Henan province (No. 24B430003) and the Doctoral Research Start-Up Fund of the Anyang Institute of Technology (No. BSJ2023003).

REFERENCES

1. **Jokari-Sheshdeh, M., Ali, Y.H., Gallo, S.C., Lin, W.K., Gates, J.D.** Comparing the Abrasion Performance of NiHard-4 and High-Cr-Mo White Cast Irons: The Effects of Chemical Composition and Microstructure *Wear* 492 – 493 2022: pp. 204208. https://doi.org/10.1016/j.wear.2021.204208
2. **Li, C., Li, Y.F., Shi, J., Li, B., Gao, Y.M., Goei, R., Li, Y.H., Shah, I.A., Wu, K., Zhao, S.Y., Yoong Tok, A.I.** Interfacial Characterization and Erosive Wear Performance of Zirconia Toughened Alumina Ceramics Particles Reinforced High Chromium White Cast Irons Composites *Tribology International* 165 2022: pp. 107262. https://doi.org/10.1016/j.triboint.2021.107262
3. **Sare, I.R.** Abrasion Resistance and Fracture Toughness of White Cast Irons *Materials Science and Technology* 19 2013: pp. 412 – 419. https://doi.org/10.1179/030716979803276228
4. **Purba, R.H., Shimizu, K., Kusumoto, K., Todaka, T., Shirai, M., Hara, H., Ito, J.** Erosive Wear Characteristics of High-Chromium Based Multi-component White Cast Irons *Tribology International* 159 2021: pp. 106982. https://doi.org/10.1016/j.triboint.2021.106982
5. **Guitar, M.A., Suárez, S., Prat, O., Guigou, M.D., Gari, V., Pereira, G., Mücklich, F.** High Chromium Cast Irons: Destabilized-Subcritical Secondary Carbide Precipitation and Its Effect on Hardness and Wear Properties *Journal of Materials Engineering and Performance* 27 2018: pp. 3877 – 3885. https://doi.org/10.1007/s11665-018-3347-1
6. **Durman, R.W.** Progress in Abrasion-Resistant Materials for Use in Comminution Processes *International Journal of Mineral Processing* 22 1988: pp. 381 – 399. https://doi.org/10.1016/0301-7516(88)90074-9
7. **Pranav Nayak, U., Mücklich, F., Guitar, M.A.** Interplay Between the Microstructure and Tribological Performance of a Destabilized 26 wt.% Cr HCCI: The Influence of Temperature and Heating Rate *Tribology International* 185 2023: pp. 108532. https://doi.org/10.1016/j.triboint.2023.108532
8. **Bergami, L.B., Lima, A.O., Venturelli, B.N., Machado, I.F., Albertin, E., Souza, R.M.** Effect of Carbide Orientation During Single Scratch Test in Directionally Solidified and Heat-Treated High Chromium Cast Irons *Wear* 523 2023: pp. 204823. https://doi.org/10.1016/j.wear.2023.204823
9. **Li, Y.C., Li, P., Wang, K., Li, H.Z., Gong, M.Y., Tong, W.P.** Microstructure and Mechanical Properties of a Mo Alloyed High Chromium Cast Iron After Different Heat Treatments *Vacuum* 156 2018: pp. 59 – 67. https://doi.org/10.1016/j.vacuum.2018.07.013
10. **Ding, H.S., Liu, S.Q., Zhang, H.L., Guo, J.J.** Improving Impact Toughness of a High Chromium Cast Iron Regarding Joint Additive of Nitrogen and Titanium *Materials & Design* 90 2016: pp. 958 – 968. https://doi.org/10.1016/j.matdes.2015.11.055
11. **Geng, B.Y., Zhou, R.F., Li, Y.K., Wang, Q.P., Jiang, Y.H.** The Difference in Effects of Electric Current Pulses on Inoculation of Austenite and M_7C_3 Carbides *Materials Research Express* 7 (9) 2020: pp. 096506. https//doi.org/10.1088/2053-1591/abb2d0
12. **Chen, C., Lv, B., Ma, H., Sun, D.Y., Zhang, F.C.** Wear Behavior and the Corresponding Work Hardening Characteristics of Hadfield Steel *Tribology International* 121 2018: pp. 389 – 399. https://doi.org/10.1016/j.triboint.2018.01.044
13. **Chen, C., lv, B., Feng, X.Y., Zhang, F.C., Beladi, H.** Strain Hardening and Nanocrystallization Behaviors in Hadfield Steel Subjected to Surface Severe Plastic Deformation *Materials Science and Engineering: A* 729 2018: pp. 178 – 184. https://doi.org/10.1016/j.msea.2018.05.059
14. **Zhang, F.C., Lv, B., Xu, A.Y.** Explosion Hardening of Hadfield Steel Crossing *Materials Science and Technology* 26 (2) 2010: pp. 223 – 232. https://doi.org/10.1179/174328408X363263
15. **Niu, L.B., Hojamberdiev, M., Xu, Y.H., Wu, H.** Microstructure and Mechanical Properties of Hadfield Steel Matrix Composite Reinforced With Oriented High-Chromium Cast Iron Bars *Journal of Materials Science* 45 2010: pp. 4532 – 4538. https://doi.org/10.1007/s10853-010-4549-6
16. **Li, J., Liu, C.Y., Song, Y.H., Zhao, G.H., Ma, L.F., Huang, Q.X.** Influence of Hot Rolling + Heat treatment on Microstructure and Mechanical Properties of NM500/Q345/NM500 Composite Plate *Journal of Materials Science* 56 2021: pp. 6016 – 6030. https://doi.org/10.1007/s10853-020-05666-4
17. **Xiong, B.W., Cai, C.C., Wan, H., Lu, B.P.** Fabrication of High Chromium Cast Iron and Medium Carbon Steel Bimetal

by Liquid–Solid Casting in Electromagnetic Induction Field *Materials & Design* 32 (5) 2011: pp. 2978 – 2982. https://doi.org/10.1016/j.matdes.2011.01.006

18. **Xiao, X.F., Ye, S.P., Yin, W.X., Xue, Q.** HCWCI/Carbon Steel Bimetal Liner by Liquid-Liquid Compound Lost Foam Casting *Journal of Iron Steel Research International* 19 2012: pp. 13 – 19. https://doi.org/10.1016/S1006-706X(12)60145-9
19. **Jilleh, A., Babu, N.K., Thota, V., Anis, A.L., Harun, M.K., Talari, M.K.** Microstructural and Wear Investigation of High Chromium White Cast Iron Hardfacing Alloys Deposited on Carbon Steel *Journal of Alloys and Compounds* 857 2021: pp. 157472. https://doi.org/10.1016/j.jallcom.2020.157472
20. **Xie, G.L., Sheng, H., Han, J.T.** Fabrication of High Chromium Cast Iron/Low Carbon Steel Composite Material by Cast and Hot Rolling Process *Materials & Design* 31 2010: pp. 3062 – 3066. https://doi.org/10.1016/j.matdes.2010.01.014
21. **Eroglu, M. Kurt, B.** Diffusion Bonding Between High Chromium White Iron and Low Carbon Steel *Materials Science and Technology* 23 2007: pp. 171 – 176. https://doi.org/10.1179/174328407X154202
22. **Li, Y.C., Gong, M.Y., Wang, K., Li, P., Yang, X., Tong, W.P.** Diffusion Behavior and Mechanical Properties of High Chromium Cast Iron/Low Carbon Steel Bimetal *Materials Science and Engineering A* 718 2018: pp. 260 – 266. https://doi.org/10.1016/j.msea.2018.01.111
23. **Liu, F., Jiang, Y.H., Xiao, H., Tan, J.** Study on Fragmentation and Dissolution Behavior of Carbide in a Hot-Rolled Hypereutectic High Chromium Cast Iron *Journal of Alloys and Compounds* 618 2015: pp. 380 – 385. https://doi.org/10.1016/j.jallcom.2014.07.131
24. **Wang, P.J., Huang, H.T., Liu, J.J., Liu, Q., Chen, Z.J.** Microstructure and Mechanical Properties of Ti6Al4V/AA6061/AZ31 Laminated Metal Composites (LMCs) Fabricated by Hot Roll Bonding *Journal of Alloys and Compounds* 861 2021: pp. 157943. https://doi.org/10.1016/j.jallcom.2020.157943
25. **Liu, P.T., Ma, L.F., Jia, W.T., Wang, T., Zhao, G.H.** Hot Deformation Behavior of a Novel Bimetal Consisting of BTW1 and Q345R Characterized by Processing Maps *Frontiers of Mechanical Engineering* 14 2019: pp. 489 – 495. https://doi.org/10.1007/s11465-019-0554-x
26. **Zheng, B.Z., Prastiti, N.G., Balint, D.S., Dunne, F.P.E.** The Dislocation Configurational Energy Density in Discrete Dislocation Plasticity *Journal of the Mechanics and Physics of Solids* 129 2019: pp. 39 – 60. https://doi.org/10.1016/j.jmps.2019.04.015